Attenuation of signaling pathways stimulated by pathologically activated FGF-receptor 2 mutants prevents craniosynostosis

V. P. Eswarakumar*, F. Özcan*†, E. D. Lew*, J. H. Bae*, F. Tomé*, C. J. Booth‡, D. J. Adams§, I. Lax*, and J. Schlessinger*¶

*Department of Pharmacology and ‡Section of Comparative Medicine, Yale University School of Medicine, New Haven, CT 06520; and §Department of Orthopaedic Surgery, University of Connecticut Health Center, Farmington, CT 06030

Contributed by J. Schlessinger, October 19, 2006 (sent for review September 22, 2006)

Craniosynostosis, the fusion of one or more of the sutures of the skull vault before the brain completes its growth, is a common (1 in 2,500 births) craniofacial abnormality, ≈20% of which occurrences are caused by gain-of-function mutations in FGF receptors (FGFRs). We describe a genetic and pharmacological approach for the treatment of a murine model system of Crouzon-like craniosynostosis induced by a dominant mutation in Fgfr2c. Using genetically modified mice, we demonstrate that premature fusion of sutures mediated by Crouzon-like activated Fgfr2c mutant is prevented by attenuation of signaling pathways by selective uncoupling between the docking protein Frs2α and activated Fgfr2c, resulting in normal skull development. We also demonstrate that attenuation of Fgfr signaling in a calvaria organ culture with an Fgfr inhibitor prevents premature fusion of sutures without adversely affecting calvaria development. These experiments show that attenuation of FGFR signaling by pharmacological intervention could be applied for the treatment of craniosynostosis or other severe bone disorders caused by mutations in FGFRs that currently have no treatment.

bone disorders | cell signaling | cell surface receptors | protein kinases | skull development

Development of the skull is a complex process regulated by signaling mechanisms that differ significantly from those required for the development of the axial (e.g., vertebral column, ribs, and sternum) and appendicular (e.g., limbs and girdles) skeletons (1). To accommodate the rapidly growing brain during the early years of life, the cranial bones grow at their fibrous joints, called sutures. These sutures contain immature rapidly dividing osteogenic stem cells. Signaling pathways activated by FGFs, bone morphogenetic proteins, TGF-β, and noggin play an important role in suture development (2–4). Craniosynostosis, the premature fusion of one or more sutures of the skull before the brain completes its growth, is one of the most common craniofacial abnormalities caused by abnormal signaling in the sutural mesenchyme. Hallmarks of craniosynostosis include abnormally shaped skull, often associated with increased intracranial pressure, mental retardation, developmental delay, seizures, and blindness caused by the constriction of the growing brain (5). Craniosynostosis occurs with a prevalence of ≈1 in 2,100–3,000 births (6), and ≈20% of all known craniosynostosis disorders are caused by gain-of-function mutations in members of the FGF receptor (FGFR) family of receptor tyrosine kinases (7). For example, mutations in *FGFR2* cause Crouzon, Apert, Pfeiffer, Jackson—Weiss, and Beare–Stevenson syndromes (reviewed in ref. 8). These diseases are caused by gain-of-function mutations in one of the two alleles of *FGFR2*, which results in ligand-independent homodimerization and activation of mutant receptors (9, 10). It is noteworthy that these patients have a normal allele of *FGFR2* in addition to the mutated allele.

The extracellular domain of FGFRs is composed of three Ig-like domains (D_1, D_2, and D_3) in which D_2 and D_3 function as FGF-and heparin-binding regions. Formation of a ternary FGF/heparin/FGFR complex results in FGFR dimerization and activation (11–14). The Crouzon Cys342Tyr mutation disrupts the structure of D_3, abrogating the ligand-binding capacity of the extracellular domain of FGFR2c. In addition, Cys-278, which normally forms an intramolecular disulfide bond with Cys-342, becomes unpaired. The unpaired Cys-278 instead forms a disulfide bond with Cys-278 of a neighboring similarly mutated FGFR2c molecule intermolecularly resulting in the formation of constitutively activated stable homodimers that are unable to bind FGF (9, 10, 15).

We have previously demonstrated that the two members of the Frs2 family of docking proteins play an important role in cell signaling by Fgfrs (16). Mice deficient in Frs2α have multiple defects in signaling by Fgfrs resulting in embryonic lethality at an early stage of gastrulation (17). To circumvent this problem and reveal the role of Frs2α in cell signaling by pathologically activated Fgfrs or specific isoforms of Fgfrs, we have generated Fgfr mutants that are not capable of recruitment and stimulation of tyrosine phosphorylation of Frs2α. Here we show that the adverse effect caused by activated Fgfr2c in Crouzon-like mutant mice can be prevented by genetic or pharmacological attenuation of Fgfr signaling.

Results and Discussion

To study the role of Frs2α in signaling by Crouzon-like Fgfr2c mutant mice, two kinds of germ-line mutations in the *Fgfr2* gene were generated. The first mutation is a Crouzon-like point mutation in the extracellular domain in which Cys-342 was replaced by a Tyr residue (Fig. 1). The second mutation in cis to the first mutation was made in the juxtamembrane domain of the same *Fgfr2c* molecule, wherein two amino acids, Leu-424 and Arg-426 (LR), were replaced by Ala residues. Biochemical and biophysical studies have demonstrated that several residues in the juxtamembrane domain, including the LR, play an important role in mediating complex formation between the phosphotyrosine-binding domain of Frs2 and the juxtamembrane domain of Fgfrs (18, 19).

Mutations in the Juxtamembrane Domain Uncouple Frs2α from Fgfr2. We first evaluated the LR mutation *in vitro* for its ability to mediate tyrosine phosphorylation of Frs2α and other signaling

CELL BIOLOGY

Author contributions: V.P.E. and J.S. designed research; V.P.E., F.Ö., E.D.L., J.H.B., F.T., C.J.B., D.J.A., and I.L. performed research; V.P.E., I.L., and J.S. analyzed data; and V.P.E. and J.S. wrote the paper.

The authors declare no conflict of interest.

Abbreviations: FGFR, FGF receptor; LR, Leu-424 and Arg-426; CLR, Cys-342, Leu-424, and Arg-426; microCT, microcomputed tomography; E*n*, embryonic day *n*; TCS, tracheal cartilaginous sleeve.

†Present address: Department of Biology, Gebze Institute of Technology, Gebze 41400, Kocaeli, Turkey.

¶To whom correspondence should be addressed. E-mail: joseph.schlessinger@yale.edu.

This article contains supporting information online at www.pnas.org/cgi/content/full/0609157103.DC1.

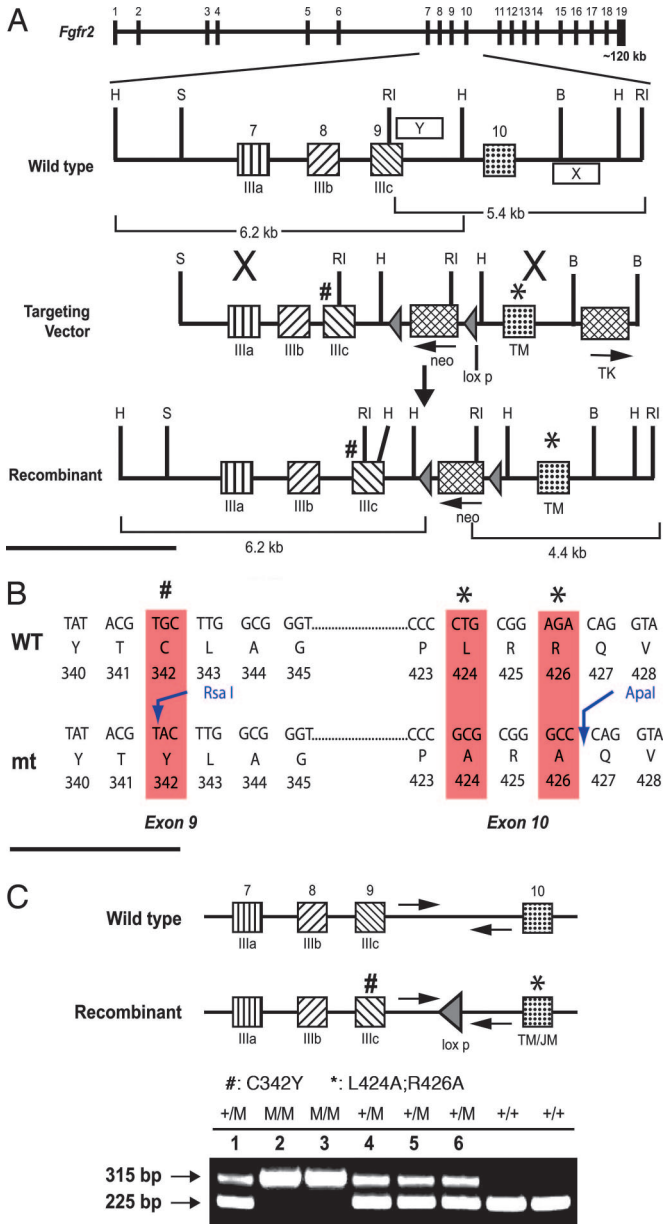

Fig. 1. Generation of targeting vector for Crouzon syndrome-like Fgfr2c mutant deficient in recruitment of FRS2α. (*A*) Schematic diagram showing the genomic structure of Fgfr2. The targeting vector contains 8.6 kb of the Fgfr2 genomic fragment, interrupted by the loxp-flanked *mc1-neo* gene inserted at the HindIII site of intron 9. A PGK-TK gene was inserted at the BamHI site of intron 10. Cys-342 was replaced by a Tyr residue in exon 9 (marked #). L424 and R426 were mutated to Alanine in exon 10 (marked *). The genomic portions used as probes for Southern blot analyses were indicated as X (3′ external probe) and Y (5′ internal probe). RI, EcoRI; H, HindIII; B, BamHI; S, SalI. (*B*) Sequences from exons 9 and 10 showing the site of mutations and the newly created restriction sites. (*C*) PCR analysis of the genotypes of newborn pups from the *Fgfr2c*$^{CLR/+}$ intercross. Arrows show the location of PCR primers. WT allele gives ≈225-bp product, and the recombinant allele gives ≈315-bp PCR product (M, CLR mutant).

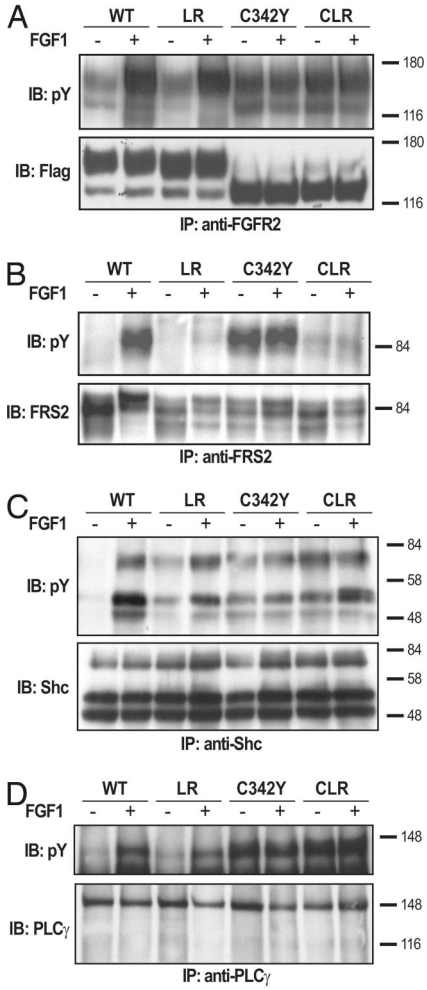

Fig. 2. Tyrosine phosphorylation of FRS2 is prevented by mutations in the juxtamembrane domain of FGFR2. L6 myoblasts devoid of endogenous FGFR expressing WT Fgfr2c, Fgfr2c-LR, -C342Y, or -CLR mutants were used in these experiments (*A–D*). A FLAG tag was inserted to the C-terminal end of all of the receptors. Serum-starved L6 myoblasts were stimulated with FGF1 for 10 min at 37°C. The cell lysates were subjected to immunoprecipitation with anti-FGFR2 antibodies (*A*), anti-FRS2 antibodies (*B*), anti-Shc antibodies (*C*), or antiphospholipase-Cγ antibodies (*D*) followed by immunoblotting with anti-pTyr antibodies. Tyrosine phosphorylation of FRS2α (*B*), Shc (*C*), and phospholipase-Cγ (*D*) in lysates from L6 cells expressing WT Fgfr2c, Fgfr2c-LR, -C342Y, or -CLR mutants are shown. As a control, blots were also probed with anti-FLAG (*A*), anti-FRS2 (*B*), anti-Shc (*C*), or anti-PLCγ (*D*) antibodies. It was previously demonstrated that the different electrophoretic mobility of the C342Y mutant is caused by altered glycosylation pattern (9). Also, note that FGF1 stimulation does not enhance the activity of Fgfr2c-C342Y and -CLR mutants (*A–D*).

proteins using a chimeric Fgfr2c molecule expressed in NIH 3T3 cells. The experiment presented in supporting information (SI Fig. 6 shows that the LR mutation prevents ligand-induced tyrosine phosphorylation of Frs2α, whereas the intrinsic tyrosine kinase activity of the receptor and tyrosine phosphorylation of Shc are retained. Because Frs2α is not tyrosine phosphorylated in cells expressing the Fgfr2-LR mutant, Grb2, Shp2, and Gab1 are not recruited by Frs2α in these cells after FGF1 stimulation (data not shown). Also, similar to the results obtained with cells derived from Frs2α-null embryos (20), FGF1 stimulation of MAPK and Akt are strongly compromised in cells expressing the Fgfr2-LR mutants (data not shown).

We have also demonstrated that the Crouzon-like Fgfr2c mutation (C342Y) expressed in L6 myoblasts, cells lacking endogenous Fgfr, enhances the tyrosine kinase activity of Fgfr2c in a ligand-independent manner. The experiment presented in Fig. 2*A* shows that the Crouzon-like Cys342Tyr Fgfr2c mutants possess constitutively activated tyrosine kinase activity, and that the addition of FGF1 has no effect on the activity of the mutant receptor. These results are consistent with previously published reports concerning the mode of action of Crouzon-like mutations (9, 10, 15). Because the Cys342Tyr mutant is displayed on

the cell surface in the form of a disulfide-bridged homodimer that cannot bind FGF, this mutant receptor is unable to form FGF-induced heterodimers with other members of the Fgfr family.

Substitution of the LR residues in the juxtamembrane domain of an activated Fgfr2c carrying a Crouzon-like mutation (designated hereafter as Fgfr2-CLR) (CLR, Cys-342, Leu-424, and Arg-426) prevents the recruitment and tyrosine phosphorylation of Frs2α (Fig. 2*B*). However, the intrinsic tyrosine kinase activity (Fig. 2*A*) and ability of the Fgfr2-CLR mutant to recruit and phosphorylate other signaling molecules, such as Shc (Fig. 2*C*) and phospholipase-Cγ (Fig. 2*D*), were unaffected by the mutations. Thus, the LR mutation in the juxtamembrane domain of Fgfr2c disrupts specifically the tyrosine phosphorylation of Frs2α without affecting other signaling pathways stimulated by FGF signaling.

Genetic Attenuation of Mutant Fgfr2c Signaling Prevents Crouzon-Like Syndrome in Mice. Mice carrying the C342Y, L424A and R426A (*Fgfr2c*$^{CLR/+}$) triple mutations were created by using the knockin gene-targeting approach. The targeting vector that contained the desired mutations in the *Fgfr2* gene (Fig. 1) was electroporated into mouse ES cells, and germ-line transmitting chimeras were made from two independent clones. The heterozygous *Fgfr2c*$^{C342Y/+}$ Crouzon-like mice are characterized by ocular proptosis (protruding eyes), rounded cranium, and severe reduction in the development of the midfacial area. Interestingly, the heterozygous *Fgfr2c*$^{CLR/+}$ mice that carry the Crouzon-like mutation in the extracellular domain of *Fgfr2c* but are unable to recruit Frs2α because of the LR mutation in the juxtamembrane domain are normal without any sign of defect in craniofacial development (Fig. 3 *A–C*). To characterize these mice further, the skulls of WT, *Fgfr2c*$^{C342Y/+}$, and *Fgfr2c*$^{CLR/+}$ mice were stained with alizarin red by using a standard protocol. All of the sutures are visible in WT and *Fgfr2c*$^{CLR/+}$ mutant mice, whereas in *Fgfr2c*$^{C342Y/+}$ mutant mice, the coronal sutures are fused with significantly shortened facial region (Fig. 3 *D–F*). The fine details of the cranial sutures were analyzed by using microcomputed tomography (microCT) imaging. The 3D images of the calvaria show that WT mice have fully opened coronal, sagittal, and lambdoid sutures. These sutures normally remain open throughout the lifespan of the mouse. However, in Crouzon-like mutant mice (*Fgfr2c*$^{C342Y/+}$), the coronal sutures are completely fused on both sides of the skull. By contrast, the premature fusion of the coronal suture is completely prevented, and the skulls of mice carrying the CLR mutation (*Fgfr2c*$^{CLR/+}$) are morphologically indistinguishable from those of WT mice (Fig. 3 *G–I*). The sutures were further examined by analyzing 2D images of the coronal suture crosssections of 6-week-old calvaria. The coronal sutures of both WT and *Fgfr2c*$^{CLR/+}$ mice remain open with overlapping ossified frontal and parietal bones, whereas the coronal sutures of Crouzon-like mutant *Fgfr2c*$^{C342Y/+}$ mice are fused (Fig. 3 *J–L*). Histological analyses of coronal sutures of 1-week-old mice revealed the presence of abundant mineralized bone trabeculae in the coronal suture mesenchyme of Crouzon-like mutant *Fgfr2c*$^{C342Y/+}$ mice, whereas the same sutures are unaffected in the *Fgfr2c*$^{CLR/+}$ mice (Fig. 3 *M–O*). In addition, inspection of calvaria at several time points during postnatal growth period using microCT revealed that the coronal sutures of *Fgfr2c*$^{CLR/+}$ mice remain open even after 1 year of postnatal life (SI Fig. 7). These results show that Frs2α is an important mediator of the signaling pathways that are responsible for development of craniosynostosis caused by activating mutations in Fgfr2c.

That the heterozygous CLR mice (*Fgfr2c*$^{CLR/+}$) did not show any signs of craniosynostosis and are phenotypically indistinguishable from WT littermates prompted us to explore the possibility of whether the LR mutation inadvertently inactivated the mutant allele *in vivo*. It has been shown that the targeted inactivation of *Fgfr2 in toto*, which leads to the inactivation of both the b and c isoforms of Fgfr2, causes an embryonic lethal phenotype at embryonic day (E)10.5, because of impairment in the development of the placenta (21). If the LR mutation inactivated the *Fgfr2* gene, the homozygous Fgfr2-CLR embryos would not survive beyond E10.5. This has been tested by intercrossing *Fgfr2c*$^{CLR/+}$ mice to generate homozygous *Fgfr2c*$^{CLR/CLR}$ mice. Genotyping of the newborn pups (SI *Supporting Text*) has shown that 25% of the offspring were homozygous *Fgfr2c*$^{CLR/CLR}$ mice (Fig. 1*C*). This shows that the LR mutation did not inactivate the *Fgfr2* gene because, otherwise, the *Fgfr2c*$^{CLR/CLR}$ embryos would not have survived beyond E10.5 (21).

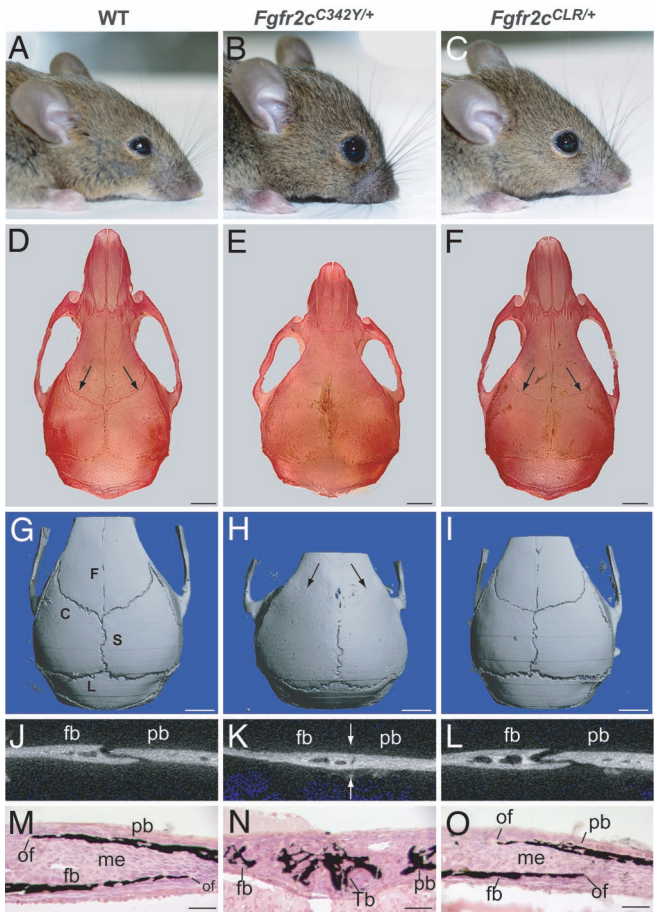

Fig. 3. Craniosynostosis is prevented by uncoupling Frs2α from Crouzon-like Fgfr2c mutant in *Fgfr2c*$^{CLR/+}$ mice. Photographs of the heads of 6-week-old live mice (*A–C*) and Alizarin-stained skulls (*D–F*). Note the open sutures in the WT and *Fgfr2c*$^{CLR/+}$ skulls (arrows); microCT scans showing 3D images of calvaria (*G–I*). Note completely fused coronal suture in *Fgfr2c*$^{C342Y/+}$ mutant mice (arrows) and open sutures in WT and *Fgfr2c*$^{CLR/+}$ mice. (*J–L*) 2D images of crosssection of coronal suture showing open suture of WT mice, fused suture of *Fgfr2c*$^{C342Y/+}$ mice (arrows) and open suture of *Fgfr2c*$^{CLR/+}$ mice. (*M–O*) Histological section of coronal sutures of 1-week-old mice stained with von Kossa and methyl green. Note the presence of bone trabeculae in the sutural mesenchyme in the *Fgfr2c*$^{C342Y/+}$ mutant. (*Left*) WT, (*Center*) *Fgfr2c*$^{C342Y/+}$, and (*Right*) *Fgfr2c*$^{CLR/+}$. C, coronal suture; S, sagittal suture; L, lambdoid suture; F, frontal suture; fb, frontal bone; pb, parietal bone; of, ossification front; me, mesenchyme; and Tb, bone trabecula. [Scale bars: 2 mm (*D–I*); 100 μm (M–O).]

FRS2α-Dependent and Independent Biological Responses in Crouzon-Like Syndrome. We next explored the Frs2α-dependent and independent biological responses of activated Fgfr2 by comparing the phenotypes of *Fgfr2c*$^{C342Y/C342Y}$ with *Fgfr2c*$^{CLR/CLR}$ mice. Because Crouzon syndrome is caused by a dominant mutation in one of the

CELL BIOLOGY

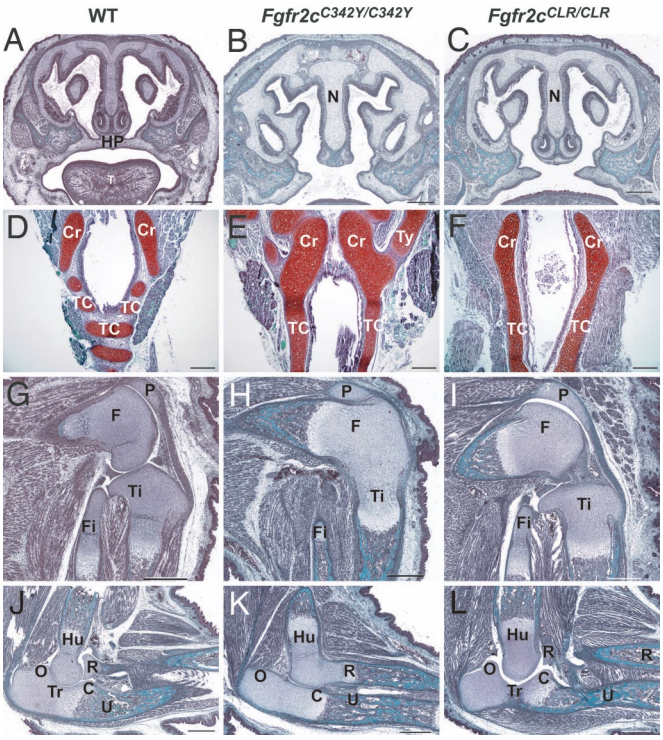

Fig. 4. Frs2α-dependent and independent biological responses in Crouzon-like syndrome. (*A–C*) Coronal sections through the head showing intact hard palate of E18.5 embryos of WT mice (*A*) and cleft palates in *Fgfr2c*$^{C342Y/C342Y}$ (*B*) and *Fgfr2c*$^{CLR/CLR}$ mice (*C*). (*D–F*) Trachea showing the cartilaginous rings in WT mice (*D*), whereas in *Fgfr2c*$^{C342Y/C342Y}$ (*E*) and *Fgfr2c*$^{CLR/CLR}$ (*F*) mice, the cricoid is not separated from the tracheal cartilage. In the mutants, there is no separation of the tracheal cartilage into rings, and the trachea appears like a smooth cartilaginous tube. (*G–I*) Knee joints of E18.5 embryos of WT mice (*G*) are similar to the knee joints of *Fgfr2c*$^{CLR/CLR}$ mutants (*I*), exhibiting normal development of the joint space. The joint spaces did not form in the *Fgfr2c*$^{C342Y/C342Y}$ mice (*H*). (*J–L*) Normal elbow joint development in WT (*J*) and *Fgfr2c*$^{CLR/CLR}$ mice (*L*). *Fgfr2c*$^{C342Y/C342Y}$ mice (*K*) exhibit joint agenesis between the humerus and radius and secondary agenesis of the coronoid process and trochelar fossa in the ulna. C, coronoid process; Cr, cricoid cartilage; F, femur; Fi, fibula; Hu, humerus; HP, hard palate; N, nasal septum; O, olecranon process; P, patella; R, radius; T, tongue; Tc, tracheal cartilage rings; Ti, tibia; Tr, trochlear notch; Ty, thyroid cartilage; and U, ulna. Staining, Mason's trichrome (*A–C* and *G–L*); Safranin O (*D–F*). (Scale bars: 200 μm.)

two alleles of the *Fgfr2* gene, both the patients and the animal model for this syndrome are heterozygous for this mutation. Homozygosity for Crouzon mutation has not been reported in humans. However, we were intrigued by the fact that homozygous Crouzon-like mutant mice (*Fgfr2c*$^{C342Y/C342Y}$) die within 1 day after birth. The death of the homozygous *Fgfr2c*$^{C342Y/C342Y}$ mice is most likely caused by a cleft in the palate (Fig. 4), which results in feeding problems. Moreover, the cartilaginous rings of the trachea of homozygous *Fgfr2c*$^{C342Y/C342Y}$ mice are not separated by fibrous membranous tissue, which leads to the formation of a continuous tube-shaped cartilaginous core known as tracheal cartilaginous sleeve (TCS; see Fig. 4). Consequently, the trachea becomes more rigid, resulting in impaired normal breathing of these mice. In addition, *Fgfr2c*$^{C342Y/C342Y}$ mice displayed agenesis of joint spaces between distal femur and proximal tibia as well as between distal humerus and proximal radius that resulted in the fused knees and elbows (Fig. 4).

Analyses of homozygous mice deficient in Frs2α recruitment (*Fgfr2c*$^{CLR/CLR}$ mice) revealed the Frs2α-dependent and -independent responses in Crouzon-like syndrome. For example, agenesis of the joint spaces at knees and elbows was fully rescued in homozygous *Fgfr2c*$^{CLR/CLR}$ mice, indicating that Frs2α is required for these phenotypes. In contrast, the cleft palate and TCS were not rescued in the homozygous *Fgfr2c*$^{CLR/CLR}$ mutant mice, demonstrating that Frs2α is dispensable for those phenotypes (Fig. 4). However, it is important to note that the cleft palate and TCS phenotypes were not caused by a compensatory mechanism that may take place as a consequence of deficiency in Frs2α recruitment, because the same phenotypes are also detected in homozygous Crouzon-like mice. If deficiency in recruitment of Frs2α in CLR mice would have led to activation of alternative compensatory pathways, one would have expected to see additional phenotypes in *Fgfr2c*$^{CLR/CLR}$ mice. However, these phenotypes were not detected in the *Fgfr2c*$^{CLR/CLR}$ mutant mice. The deficiency of the Fgfr2 to recruit Frs2α is not compensated by heterodimerization with other FGFRs, because the Fgfr2c-CLR mutant is displayed on the cell surface in the form of a disulfide-bridged homodimer that has lost the capacity to bind FGF.

These results demonstrate that the cleft palate and TCS phenotypes in Crouzon-like syndrome are mediated by Frs2α-independent cell signaling pathway(s). The Frs2α-independent response could be mediated by other signaling molecules that lie downstream of Fgfrs, including Shc, PLCγ, or Stat1 (22, 23). It was recently reported that an Fgfr1 mutant deficient in Frs2α recruitment is also able to mediate Frs2α-independent cellular responses (24).

Pharmacological Attenuation of FGFR2 Signaling. Pharmacological interventions that would interfere with the interactions between the phosphotyrosine-binding domain of Frs2α and the juxtamembrane domain of Fgfr2c could be considered for the treatment of Crouzon syndrome and other craniofacial disorders caused by activated forms of Fgfrs. However, unlike the genetic approach that enables selective attenuation of signaling by the activated Crouzon-like Fgfr2c mutant, pharmacological agents that interfere with complex formation between the phosphotyrosine-binding domain of Frs2α and Fgfr2c will not distinguish between mutant and WT receptors. An alternative approach that also will not distinguish between mutant and WT receptors is to apply a protein tyrosine kinase inhibitor that inhibits the activity and action of Fgfrs.

Tyrosine kinase inhibitors have been successfully applied for the treatment of diseases, such as chronic myelogenous leukemia and gastrointestinal stromal tumors, caused by activated forms of tyrosine kinases. In both cases, resistance toward the tyrosine kinase inhibitor STI571 was conferred by mutations in the tyrosine kinase domain of Abl (25). Because of the problem of drug resistance, it is important to generate a variety of FGFR inhibitors belonging to different classes of chemical scaffold (26). We have used a previously undescribed small-molecule inhibitor of FGFR, [4-(3,5-difluorophenyl)-1*H*-pyrrolo[2,3-b]pyridin-3-yl](3-methoxyphenyl) methanone (PLX052), to attenuate signaling of mutant Fgfr2 in a calvaria organ culture. Full details about the synthesis of this compound will be described elsewhere. The mechanism of inhibition, dose-response, and cocrystal structure with Fgfr1 kinase domain were described in SI Figs. 8 and 9 as well as SI Table 1.

We next applied PLX052 for the treatment of newborn Crouzon-like *Fgfr2c*$^{C342Y/+}$ mice and control WT newborn mice. Because of its poor solubility in water, PLX052 was dissolved in buffer containing 5% DMSO. Unfortunately, newborn mice were very sensitive to injections of a buffer containing the DMSO vehicle alone. To determine whether Fgfr inhibitors show efficacy for the treatment of premature suture fusion before formulation of PLX052 is improved or a more soluble derivatives are identified, we developed and applied a calvaria organ culture system that replicates the phenotypes of WT or Crouzon-like mutant mice in culture. This system enables the

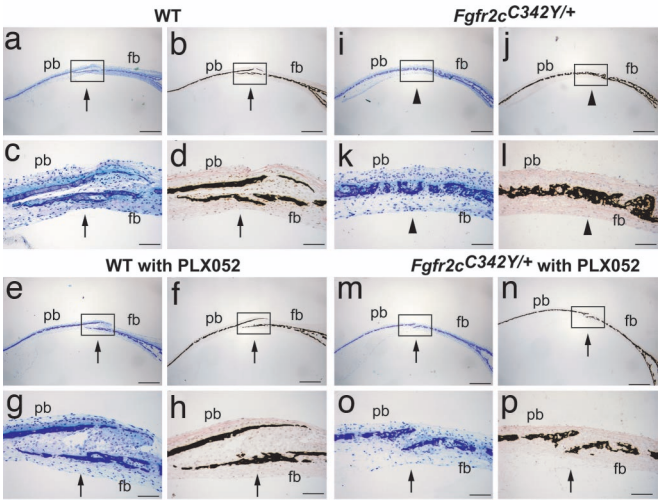

Fig. 5. Suture fusion in calvaria tissue explants is prevented by treatment with FGFR inhibitor. Calvaria harvested from E18.5-day-old embryos of WT (*a–h*) and *Fgfr2c*$^{C342Y/+}$ mutant (*i–p*) mice were cultured either with vehicle (0.2% DMSO) alone (*a–d* and *i–l*) or with 1 μM PLX052 (e–*h* and *m–p*) for 2 weeks. Histological sections of cultured calvaria were made perpendicular to the coronal suture, which passes through the frontal bone (fb) and the parietal bone (pb). Sections were stained with toluidine blue (*a*, *c*, *e*, *g*, *i*, *k*, *m*, and *o*), and adjacent sections were stained by von Kossa followed by methyl green counter staining (*b*, *d*, *f*, *h*, *j*, *l*, *n*, and *p*). *Lower* [*c*, *d*, *g*, *h*, *k*, *l*, *o*, and *p* (Scale bars: 100 μm)] depicts the higher magnification of the coronal sutures shown in the boxed regions of *Upper* [*a*, *b*, *e*, *f*, *i*, *j*, *m*, and *n* (Scale bars: 500 μm)], respectively. Open (arrow) and fused coronal sutures (arrowhead) are indicated. Fused sutures are observed in untreated calvaria from mutant mice (*i–l*), and open sutures are observed in calvaria from mutant mice treated with PLX052 (*m–p*).

analysis of the effects of pharmacological agents that interfere with the kinase activity of Fgfr on craniosynostosis in organ culture. Calvaria harvested from E18.5 day embryos of WT and Crouzon-like mutant mice were cultured in DMEM containing 10% FCS supplemented with ascorbic acid at 100 μg/ml in 24-well plates, as described (27). The experiment presented in Fig. 5 shows that the sutures of calvaria from Crouzon-like mice were fused within 2 weeks of organ culture, whereas the sutures of calvaria from WT mice remained open for as long as the calvaria were maintained in culture. The micrographs of stained sutures that are presented in Fig. 5 show that continuous treatment with 1 μM PLX052 prevented the premature fusion of coronal suture in calvaria from Crouzon-like mice. The growth and development of the sutures of WT mice, on the other hand, were not affected by treatment with 1 μM PLX052. Treatment with 5 μM PLX052 also prevented the premature fusion of coronal suture of mutant mice calvaria without affecting the normal development of the sutures in calvaria from WT mice (SI Fig. 10). For each concentration of PLX052, six calvaria samples were used, and similar results were obtained. However, when cultures were treated with 50 μM or higher concentrations of PLX052, extensive cell death was observed (data not shown). We conclude that, when applied in a certain range of concentration, PLX052 is capable of attenuating the signal emanating from the activated Crouzon-like Fgfr2c mutant to prevent premature suture fusion, and that the attenuated signal transmitted from the normal Fgfr2c allele under these conditions still permits undisturbed suture growth and development.

Conclusion

We describe genetic and pharmacological approaches that offer new opportunities for treatment of craniosynostosis and other severe bone disorders caused by gain-of-function mutations in FGFRs. Similar strategies could also be applied for the treatment of cancers driven by oncogenic mutations in FGFR1, -2, or -3 (28).

The mutation in Fgfr2c that is responsible for Crouzon syndrome is a gain-of-function mutation encoding for a ligand-independent disulfide-bridged activated form of Fgfr2c. We have, therefore, embarked on the identification of genetic and pharmacological approaches that, on the one hand, will enable attenuation of the signaling pathways stimulated by the mutated activated form of Fgfr2c and, on the other hand, will not adversely affect the activity of normal Fgfr2c and other Fgfrs required for normal development of the skull and other organs. Uncoupling of Frs2α from Crouzon-like activating mutant Fgfr2c, as in the case of *Fgfr2c*$^{CLR/+}$ mice, results in complete rescue of craniosynostosis. This experiment demonstrates that signaling pathways mediated by Frs2α play a critical role in mediating the adverse effects caused by the Crouzon mutation, and that selective attenuation of Frs2α-dependent signaling pathways transmitted by the constitutively activated mutant Fgfr2c could be applied for the treatment of craniosynostosis.

We have developed a calvaria explant culture system that replicates the phenotypes of Crouzon-like mice. Although the sutures of WT mice remain open during the duration of the experiments, the sutures of Crouzon-like mice fused within 2 weeks of maintaining the calvaria explants. The calvaria explant provides a good system for testing the effects of inhibitors that attenuate signaling by Fgfrs on the development and integrity of calvaria from mutant or WT mice. Treatment of calvaria explants derived from Crouzon-like mice with a certain range of concentrations of PLX052 prevented the premature fusion of sutures without interfering with the signaling pathways emanating from the WT allele of Fgfr2c that is required for normal suture development. Likewise, treatment of calvaria explants from WT mice with similar doses of PLX052 did not influence the integrity of suture formation, indicating that a sufficient amount of signal is transmitted from WT Fgfr2c in the presence of the inhibitor to enable normal calvaria development. Therefore, in principle, FGFR inhibitors could be used ectopically to prevent premature suture fusion and also refusion of surgically corrected previously fused sutures, a recurrent problem in treating craniosynostosis patients.

The experiments presented in this report provide both genetic and pharmacological evidence that modalities that attenuate signaling pathways stimulated by pathologically activated FGFRs could be applied for treatment of craniosynostosis and other severe bone deformities caused by activated FGFR mutants (8), which currently do not have any treatments.

Materials and Methods

Generation of *Fgfr2*$^{CLR/+}$ Knockin Mice. A mouse genomic fragment derived from 129SvJ, including exons 7–10 of *Fgfr2*, was used to create C342Y, L424A, and R426A mutations using the "Gene Editor" kit (Promega, Madison, WI). The mutagenized fragments were inserted into the "Osdupdel" vector (gift from Oliver Smithies, University of North Carolina, Chapel Hill). The targeting vector was linearized by NotI and electroporated into W9.5 ES cells. Two hundred clones resistant to G418 and Gancyclovir were screened by Southern blot hybridization for targeting events. Two of eight correctly recombined ES clones were used to make chimeras. The floxed neocassette was removed *in vivo* from the germ-line transmitting chimeras by mating to the PGK-Cre^{m} transgenic deleter strain (29).

Cell Culture, Immunoprecipitation, and Immunoblotting Experiments. A mammalian retroviral vector, pBABE, containing a puromycin resistance gene was used for expressing Fgfr2 and the various Fgfr2 mutants in NIH 3T3 and L-6 myoblast cells. Cells expressing WT or Fgfr mutants were serum-starved overnight and

ligand-stimulated. Cell lysates were subjected to immunoprecipitation followed by immunoblotting with different antibodies. Anti-mouse HRP and ProteinA-HRP were purchased from Santa Cruz Biotechnology (Santa Cruz, CA). Anti-FLAG antibodies (M2) were obtained from Sigma (St. Louis, MO).

X-Ray microCT. 3D images of skull vault sutures were acquired by using x-ray microCT (μCT40, Scanco Medical, Bassersdorf, Switzerland).

Calvaria Organ Culture. Calvaria harvested from WT or Crouzon mutant E18.5-day-old embryos were cultured in DMEM containing 10% FCS supplemented with ascorbic acid at 100 μg/ml in 24-well plates, as described (27). Medium was changed on alternate days, along with the FGFR tyrosine kinase inhibitor PLX052. Controls were cultured with vehicle only (0.2% DMSO). Calvaria were cultured for 14–21 days and then fixed in 10% buffered formalin and dehydrated followed by infiltration and embedding in methylmethacrylate plastic. Four micrometer-thick sections were collected and stained with toluidine blue. Adjacent sections were stained for minerals using von Kossa followed by methyl green counter staining.

This report is dedicated to the memory of Dr. Peter Lonai from Rehovot, Israel. We thank P. Ibrahim and P. Hirth from Plexxikon, Berkeley, CA, for PLX052. We thank Yale Core Center for Musculoskeletal Disorders (YCCMD) and Yale Transgenic Animal Facility for excellent service. We acknowledge support of the Core Center for Musculoskeletal Disorders Grant P30 AR46026 from National Institute of Arthritis and Musculoskeletal and Skin Diseases to the University of Connecticut Health Center MicroCT Facility. F. Özcan was supported by a TÜBiTAK and Nato-B1 fellowship. This work was supported by National Institutes of Health Grants R01-AR 051448 (to J.S.), R01-AR 051886 (to J.S.), and from the Pilot and Feasibility Award from the Yale Core Center for Musculoskeletal Disorders National Institutes of Health National Institute of Arthritis and Musculoskeletal and Skin Diseases Grant AR46032 (to V.P.E.).

1. Helms JA, Schneider RA (2003) *Nature* 423:326–331.
2. Kim HJ, Rice DP, Kettunen PJ, Thesleff I (1998) *Development (Cambridge, UK)* 125:1241–1251.
3. Cohen MM, Jr (1997) *J Bone Miner Res* 12:322–331.
4. Warren SM, Brunet LJ, Harland RM, Economides AN, Longaker MT (2003) *Nature* 422:625–629.
5. Nuckolls GH, Shum L, Slavkin HC (1999) *Cleft Palate Craniofac J* 36:12–26.
6. Hehr U, Muenke M (1999) *Mol Genet Metab* 68:139–151.
7. Passos-Bueno MR, Wilcox WR, Jabs EW, Sertie AL, Alonso LG, Kitoh H (1999) *Hum Mutat* 14:115–125.
8. Eswarakumar VP, Lax I, Schlessinger J (2005) *Cytokine Growth Factor Rev* 16:139–149.
9. Mangasarian K, Li Y, Mansukhani A, Basilico C (1997) *J Cell Physiol* 172:117–125.
10. Robertson SC, Meyer AN, Hart KC, Galvin BD, Webster MK, Donoghue DJ (1998) *Proc Natl Acad Sci USA* 95:4567–4572.
11. Schlessinger J, Plotnikov AN, Ibrahimi OA, Eliseenkova AV, Yeh BK, Yayon A, Linhardt RJ, Mohammadi M (2000) *Mol Cell* 6:743–750.
12. Plotnikov AN, Hubbard SR, Schlessinger J, Mohammadi M (2000) *Cell* 101:413–424.
13. Plotnikov AN, Schlessinger J, Hubbard SR, Mohammadi M (1999) *Cell* 98:641–650.
14. Spivak-Kroizman T, Lemmon MA, Dikic I, Ladbury JE, Pinchasi D, Huang J, Jaye M, Crumley G, Schlessinger J, Lax I (1994) *Cell* 79:1015–1024.
15. Galvin BD, Hart KC, Meyer AN, Webster MK, Donoghue DJ (1996) *Proc Natl Acad Sci USA* 93:7894–7899.
16. Kouhara H, Hadari YR, Spivak-Kroizman T, Schilling J, Bar-Sagi D, Lax I, Schlessinger J (1997) *Cell* 89:693–702.
17. Gotoh N, Manova K, Tanaka S, Murohashi M, Hadari Y, Lee A, Hamada Y, Hiroe T, Ito M, Kurihara T, *et al.* (2005) *Mol Cell Biol* 25:4105–4116.
18. Ong SH, Guy GR, Hadari YR, Laks S, Gotoh N, Schlessinger J, Lax I (2000) *Mol Cell Biol* 20:979–989.
19. Dhalluin C, Yan KS, Plotnikova O, Lee KW, Zeng L, Kuti M, Mujtaba S, Goldfarb MP, Zhou MM (2000) *Mol Cell* 6:921–929.
20. Hadari YR, Gotoh N, Kouhara H, Lax I, Schlessinger J (2001) *Proc Natl Acad Sci USA* 98:8578–8583.
21. Xu X, Weinstein M, Li C, Naski M, Cohen RI, Ornitz DM, Leder P, Deng C (1998) *Development (Cambridge, UK)* 125:753–765.
22. Eswarakumar VP, Horowitz MC, Locklin R, Morriss-Kay GM, Lonai P (2004) *Proc Natl Acad Sci USA* 101:12555–12560.
23. Dailey L, Ambrosetti D, Mansukhani A, Basilico C (2005) *Cytokine Growth Factor Rev* 16:233–247.
24. Hoch RV, Soriano P (2006) *Development (Cambridge, UK)* 133:663–673.
25. Shah NP, Nicoll JM, Nagar B, Gorre ME, Paquette RL, Kuriyan J, Sawyers CL (2002) *Cancer Cell* 2:117–125.
26. Mohammadi M, Froum S, Hamby JM, Schroeder MC, Panek RL, Lu GH, Eliseenkova AV, Green D, Schlessinger J, Hubbard SR (1998) *EMBO J* 17:5896–5904.
27. Opperman LA, Nolen AA, Ogle RC (1997) *J Bone Miner Res* 12:301–310.
28. Grose R, Dickson C (2005) *Cytokine Growth Factor Rev* 16:179–186.
29. Lallemand Y, Luria V, Haffner-Krausz R, Lonai P (1998) *Transgenic Res* 7:105–112.